https://doi.org/10.5194/essd-2020-313
Preprint. Discussion started: 12 January 2021

Open Access Earth System Science Data Discussions

A new dataset of river flood hazard maps for Europe and the Mediterranean Basin region

Francesco Dottori[1], Lorenzo Alfieri[2], Alessandra Bianchi[3], Jon Skoien[1], Peter Salamon[1]

1: European Commission, Joint Research Centre, Via E. Fermi 2749, 21027 Ispra, Italy.
2: CIMA Research Foundation, Savona, Italy
3: FINCONS SPA, Italy

Correspondence to: francesco.dottori@ec.europa.eu

Keywords: river flooding, flood hazard mapping, Europe, EFAS, Mediterranean Basin region.

Abstract

Continental scale hazard maps for riverine floods have grown in importance in the last years. Nowadays, they are used for a variety of research and commercial activities, such as evaluating present and future risk scenarios and adaptation strategies, as well as a support of national and local flood risk management plans. Here, we present a new set of hazard maps for river flooding that covers most of the geographical Europe and all the river basins entering the Mediterranean and Black Seas in the Caucasus, Middle East and Northern Africa countries. Maps represent inundation along 329'000 km of river network at 100 m resolution, for six different flood return periods. The input river flow data is produced by the hydrological model LISFLOOD, while inundation simulations are performed with the 2D hydrodynamic modelling LISFLOOD-FP. To provide an overview of the skill of the new maps, we undertake a detailed validation exercise of the new maps using official hazard maps for Hungary, Italy, Norway, Spain and the United Kingdom. We find that modelled maps can identify on average two-thirds of reference flood extent, however they also overestimate flood-prone areas for flood probabilities below 1-in-100-year, while for return periods equal or above 500 years the maps can correctly identify more than half of flooded areas. We attribute the observed skill to a number of shortcomings of the modelling framework, such as the absence of flood protections and rivers with upstream area

https://doi.org/10.5194/essd-2020-313
Preprint. Discussion started: 12 January 2021

below 500 km^2, and the limitations in representing river channels and topography of low land areas. In addition, the large variability of reference maps affects the correct identification of the areas for the validation, thus penalizing scores. However, modelled maps achieve comparable results to existing large-scale flood models when using similar parameters for the validation. We conclude that recently released high-resolution elevation datasets combined with reliable data of river channel geometry may greatly contribute to improve future versions of continental-scale flood hazard maps. The database is available for download at https://data.jrc.ec.europa.eu/dataset/1d128b6c-a4ee-4858-9e34-6210707f3c81 (Dottori et al., 2020a).

https://doi.org/10.5194/essd-2020-313
Preprint. Discussion started: 12 January 2021

1) Introduction

Nowadays, flood hazard maps are a basic component of any flood risk management strategy (EC 2007). They provide spatial information about a number of variables (such as flood extent, water depth, flow velocity) that are crucial to quantify flood impacts and therefore to evaluate flood risk. Moreover, they can be used as a powerful communication tool, allowing to quickly visualize the potential spatial impact of a river flood over an area.

Continental-scale and global-scale flood maps have grown in importance in the last years, and they are now used for a variety of research, humanitarian and commercial activities, and as a support of national and local flood management (Ward et al., 2015; Trigg et al., 2016). Global flood maps are used to provide flood risk information and support decision-making in spatial and infrastructure planning in countries where national level assessments are not available (Ward et al., 2015). Moreover, continental and global maps are vital for consistent quantification of flood risk and in projecting the impacts of climate change (Alfieri et al., 2015; Trigg et al., 2016; Dottori et al., 2018), allowing for comparisons between different regions, countries and river basins (Alfieri et al., 2016). Quantitative and comparable flood risk assessments are also necessary to derive measurable indicators of the targets set by international agreements such as the Sendai Framework for Disaster Risk Reduction (UNISDR, 2015).

In Europe, continental-scale flood hazard maps have been produced by Barredo et al. (2007), Feyen et al. (2012), Alfieri et al., (2014; 2015) and Paprotny et al., (2017). These maps have been used for a variety of studies, such as the evaluation of river flood risk under future socio-economic and climate scenarios (Barredo et al.,2007; Feyen et al., 2012; Alfieri et al., 2015), the evaluation of flood adaptation measures (Alfieri et al., 2016) and near-real time rapid risk assessment (Dottori et al., 2017).

The quality of continental-scale flood maps is constantly improving thanks to the increasing accuracy of datasets and modelling tools. Wing et al., (2017) developed a dataset of flood hazard maps for the conterminous United States using detailed national datasets and high-resolution hydrodynamic modelling, and demonstrated that continental-scale maps can achieve an accuracy similar to official national hazard maps, including maps based on accurate local-scale studies. Moreover, Wing et al. used the same official hazard maps to evaluate the performance of the global flood hazard model developed by Sampson et al. (2015). While the global model was less accurate than continental model, it could correctly identify over two-

https://doi.org/10.5194/essd-2020-313
Preprint. Discussion started: 12 January 2021


Open Access Earth System Science Data Discussions

thirds of flood extent. Conversely, European-scale maps have undergone limited testing against official hazard maps, due to limitations in accessing official data (Alfieri et al., 2014).

Here, we present a new set of flood hazard maps at 100m resolution (Dottori et al., 2020a), developed as a component of the Copernicus European Flood Awareness System (EFAS, www.efas.eu) to update the previous map catalogue developed by Dottori et al (2016a). The geographical extent of the new maps spans across geographical Europe (with the exclusion of the Volga river basin), and include all the rivers entering the Mediterranean Sea and the Black Sea (with the partial inclusion of the Nile river basin), plus Turkey, Syria and the Caucasus region. The hydrological input is calculated using the latest version of the LISFLOOD hydrological model (van der Knijff et al., 2010; Burek et al, 2013; https://ec-jrc.github.io/lisflood/), while flood simulations are performed with the hydrodynamic model LISFLOOD-FP, following the approach developed by Alfieri et al., (2014; 2015).

To provide a comprehensive overview of the skill of the new maps, we perform a validation exercise using official hazard maps for a number of countries, regions and large river basins in Europe. Moreover, we discuss the results of the validation in light of previous literature studies, we compare the performance of the present and previous version of the flood map dataset, and we discuss a number of tests with alternative datasets and methods.

2) Data and methods

In this Section we describe the procedure adopted to produce and validate the flood hazard maps. The hydrological input consists of daily river flow for the years 1990-2016. It was produced with the latest version of the hydrological model LISFLOOD (Section 2.1), based on interpolated daily meteorological observations. River flow data are analysed to derive frequency distributions, peak discharges and flood hydrographs that are used to simulate flooding processes at local scale with the LISFLOOD-FP hydrodynamic model, as explained in Section 2.2. Finally, Section 2.3 describes the validation exercise and the comparison of different approaches and input datasets.

2.1 The LISFLOOD model

LISFLOOD (Burek et al, 2013; van der Knijff et al., 2010) is a distributed, physically-based rainfall-runoff model combined with a routing module for river channels. In this work we use

https://doi.org/10.5194/essd-2020-313
Preprint. Discussion started: 12 January 2021


Open Access Earth System Science Data Discussions

the latest updated version of LISFLOOD, released as open-source software and available at https://ec-jrc.github.io/lisflood/. The model is applied to run a long-term hydrological simulation for the period 1990-2016 at 5 km grid spacing and daily resolution, which provides the hydrological input for the flood simulations. Note that the same simulation also provides initial conditions for daily flood forecast issued by EFAS.

The meteorological input is based on interpolated data of meteorological stations and gridded precipitation datasets (Arnal et al., 2019). Both the meteorological input and the LISFLOOD static input maps (land cover, digital elevation model, drainage network, soil parameters, parameterization of reservoirs) have been updated and expanded in respect to the simulations used in the previous flood map catalogue by Dottori et al. (2016a).

The current LISFLOOD version also benefits from an updated calibration at European scale, based on the Evolutionary Algorithm approach (Hirpa et al., 2018) with the modified Kling-Gupta efficiency criteria (KGE; Gupta et al., 2009) as objective function, and streamflow data for 1990-2016 from more than 700 gauge stations. The results of the calibration and the LISFLOOD hydrological skill are described in Arnal et al (2019), and summarized in the Appendix A. We did not carry out a formal comparison with the previous LISFLOOD calibration, which used a different algorithm and performance indicators (Zajac et al., 2013), however the larger dataset of streamflow observations and the improvement of the calibration routines should provide a better performance.

The geographical extent used in the present study to produce the flood maps follows the recent enlargement of EFAS (Arnal et al., 2019), and it is shown in Figure 1. The new domain is approximately 8’930’000 km^2 wide (an increase of 76% in respect with the previous extent) and cover the entire geographical Europe (with the exclusion of the Volga river basin and a number of river basins of the Arctic Sea in Russia), all the rivers entering the Mediterranean and Black Seas (with a partial inclusion of the Nile river basin), plus the entire territories of Armenia, Georgia, Turkey, and most of Syria and Azerbaijan. The river network included in the new flood hazard maps has a total length of 329’000 km, with an 80% increase compared to the previous flood maps (Alfieri et al., 2015; Dottori et al., 2016a).

https://doi.org/10.5194/essd-2020-313
Preprint. Discussion started: 12 January 2021

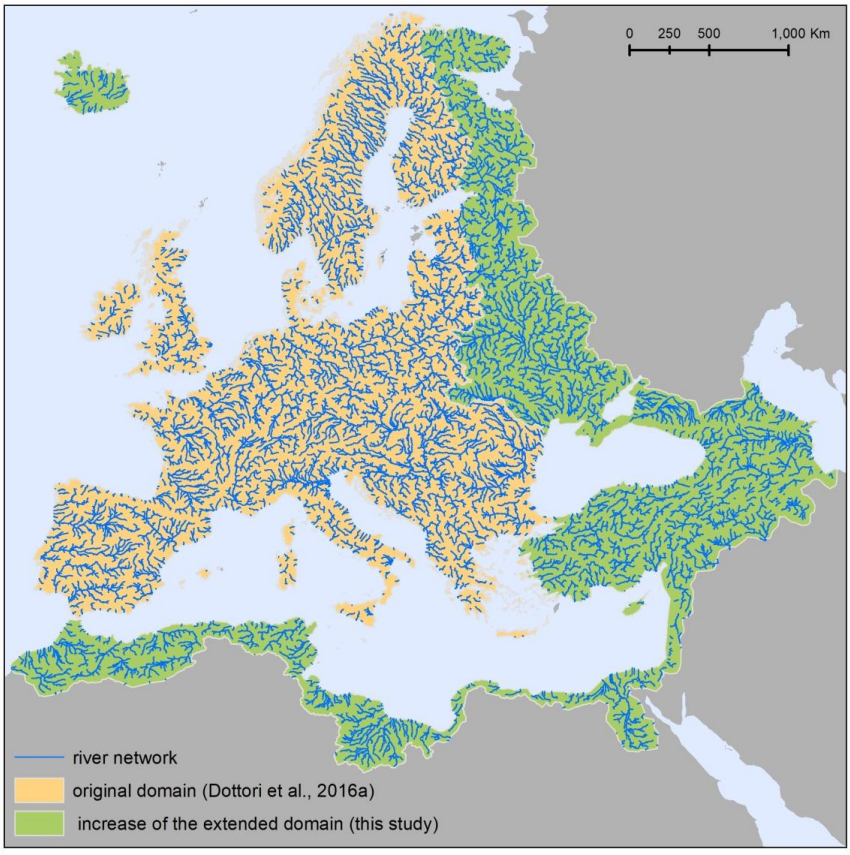

Figure 1. Geographical extent of the EFAS extended domain covered by the present dataset of flood hazard maps. The extent of the map dataset produced by Dottori et al. (2016a) is depicted in beige, while the regions added with the extended domain are in green. The figure also displays the river network considered by the flood maps.

2.2 Flood hazard mapping

The continental scale flood hazard maps presented in this study are derived from a catalogue of flood inundation maps, covering all of the EFAS river network. We briefly describe here the procedure for creating the catalogue, while the complete description can be found in Alfieri et al. (2014) and Dottori et al. (2017).

The hydrological input for creating the map catalogue is derived from the streamflow dataset of the EFAS long-term simulation, described in Section 2.1. The information is available for the

https://doi.org/10.5194/essd-2020-313
Preprint. Discussion started: 12 January 2021


Open Access Earth System Science Data Discussions

EFAS river network at 5 km grid spacing for rivers with upstream drainage areas larger than 500 km^2. We use a statistical analysis of extreme values to derive peak discharges for every cell of the river network for reference return periods of 10, 20, 50, 100, 200, 500 and 1000 years (the latter return period is use in a limited part of the model domain to allow validation against official hazard maps, see Section 2.3). In addition, we extract flow duration curves from the reference simulation, which are used together with peak discharges to calculate synthetic flood hydrographs (see Alfieri et al., 2014 for a detailed description).

The streamflow data are then downscaled to a high-resolution river network (100 m), where reference sections are identified at regular spacing along the stream-wise direction every 5 km. Each section at 100 m resolution is then linked to a section of the 5km river network, to assign a synthetic discharge hydrograph to each of them. Where the coarse- and high-resolution river networks do not overlap, flood points are linked with the closest 5km pixel in the upstream direction. Note that the match between 5 km and 100 m river sections is not always univocal. In particular, some 5 km sections have no related sections in the 100 m river network, while others can have more than one. Figure 2 shows a conceptual scheme of the two river networks. The 100m river network is included as a separate map in the dataset, to delineate which water courses have been considered in the creation of the flood hazard maps. The digital elevation model (DEM) used to derive the 100 m river network is a component of the Catchment Characterization and Modelling Database (CCM) developed at the JRC (Vogt et al., 2007). We also use a mosaic of Corine Land Cover for the year 2016 (Copernicus LMS, 2017) and GlobCover for the year 2009 (Bontemps et al., 2009) to estimate the friction coefficient based on land use.

The CCM DEM is used also to run flood simulations at 100 m resolution for each 100 m river-section using the 2D hydrodynamic model LISFLOOD-FP (Bates et al., 2010), fed with synthetic hydrographs. Therefore, for every 100 m river section we derive flood maps for the six reference return periods.

The flood maps related to the same EFAS river section (i.e. pixel of the 5 km river network) are merged together, to identify the areas at risk of flooding due to overflowing from a specific EFAS river section, and archived in the flood map catalogue. The merging is performed separately for each return period, to relate flooded areas with the magnitude of the flood event.

https://doi.org/10.5194/essd-2020-313
Preprint. Discussion started: 12 January 2021

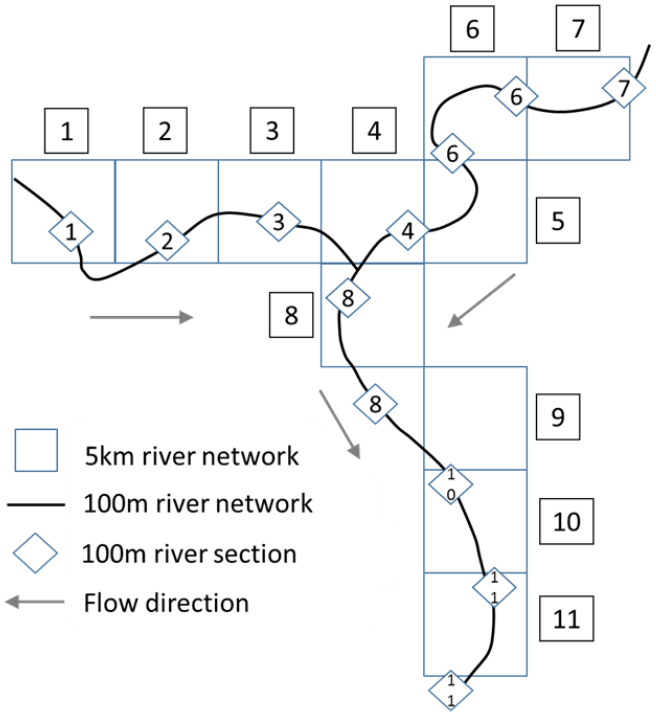

Figure 2. Conceptual scheme of the EFAS river network (5 km, squares) with the high-resolution network (100 m) and river sections (diamonds) where flood simulations are derived. The related sections of the two networks are indicated by the same number. Source: Dottori et al. (2017).

It is important to note that the flood maps developed do not take into account the influence of local flood defences, in particular dyke systems. Such limitation has been dictated mainly by the absence of consistent data at European scale. None of the available DEMs for Europe have the necessary accuracy and resolution to embed artificial embankments into elevation data. Moreover, there are no publicly available continental or national datasets describing the location and characteristics (e.g. dyke height, distance from river channel) of flood protections. Currently available datasets are based on the design return period of flood protection, e.g. the maximum return period of flood events that protections can withstand before being overflown, (Jongman et al., 2014; Scussolini et al., 2016). Most of the protection standards reported by these datasets for Europe are based on empirical regressions derived using proxy variables (e.g. gross domestic product, land use), with few data based on actual design standards. While these

https://doi.org/10.5194/essd-2020-313
Preprint. Discussion started: 12 January 2021

datasets have been applied to calculate flood risk scenarios (Alfieri et al., 2015) and flood impacts (Dottori et al., 2017), they have important limitations when used for mapping flood extent. Wing et al. (2017) linked the flood return period of protection standards with flood frequency analysis to adjust the bank height of the river channels, however with impaired performance of the model. Moreover, recent studies for United States suggest that empirical regressions based on gross domestic product and land use may not be reliable (Wing et al., 2019).

Despite these limitations, maps not accounting for physical flood defences may be applied to estimate the flood hazard in case of failure of the protection structures, and for flood events exceeding protections levels.

2.3 Validation of flood hazard maps

2.3.1 Selection of validation areas and maps

The validation of large-scale flood hazard maps requires the use of benchmarks with one or more datasets with extension and accuracy commensurate to the modelled maps. For instance Wing et al. (2017) used the official hazard maps developed for the conterminous United States to evaluate the performance of two flood hazard models, respectively designed to produce global-scale and continental-scale flood maps (see Introduction). In Europe, all member states of the European Union as well as the United Kingdom have developed national datasets of flood hazard maps for a range of flood probabilities (usually expressed with the flood return period), following the guidelines of the EU Floods Directive (EC 2007). While these maps are generally available online for consultation on Web-GIS services, only few countries and river basin authorities make the maps available for download in a format that allows comparison with geospatial data. Table 1 presents the list of flood hazard maps that could be retrieved and used for the validation exercise, while Figure 3 shows their geographical distribution. Even though more official maps are likely to become available in the near future, the maps here considered offer an acceptable overview of the different climatic zones and floodplain characteristics of the European continent. In Norway, Spain, the United Kingdom and the Po River Basin the official maps take into account flood defences, which are instead not represented in the modelling framework. To avoid over-penalizing the comparison with modelled maps, in these areas we

https://doi.org/10.5194/essd-2020-313
Preprint. Discussion started: 12 January 2021

use available maps for return periods at least 100 years or above, for which flood extent is likely to be less conditioned by flood defences.

Country	**Geographical extent**	**Return periods used**	**Defences included**
Hungary	Country scale	30 – 100 - 1000 years	No
Italy	Po River Basin	500 years	Yes
Norway	Country scale	100 years	Yes
Spain	Country scale	10 -100 - 500 years	Yes
United Kingdom	England	100 - 1000 years	Yes

Table 1. List and characteristics of the flood hazard maps used in the validation exercise.

https://doi.org/10.5194/essd-2020-313
Preprint. Discussion started: 12 January 2021

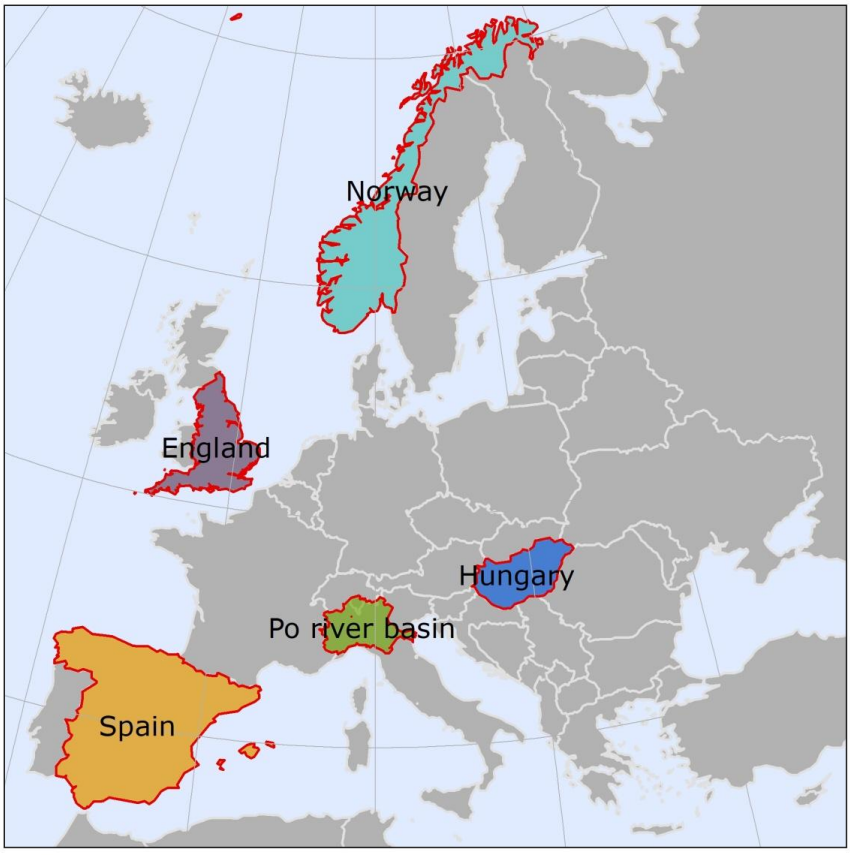

Figure 3. Geographical distribution of the test areas.

2.3.2 Performance indices and validation procedure

The national flood hazard maps listed in Table 1 are provided as polygons of flood extent, with no information on water depth. As such, official reference maps have been converted to raster format with the same resolution as the modelled maps, while the latter have been converted to binary flood extent maps. To improve the comparison between modelled and reference maps we applied a number of corrections. First, we used the CORINE Land Cover map to exclude permanent water bodies (river beds of large rivers or estuaries, lakes, reservoirs, coastal lagoons) from the comparison. Second, we restricted the comparison area around modelled maps to exclude the elements of river network (e.g. minor tributaries) included in the reference maps but not in the modelled maps. We used a different buffer extent according to each study

https://doi.org/10.5194/essd-2020-313
Preprint. Discussion started: 12 January 2021

area, considering the floodplain morphology and the variable extent and density of mapped river network. For instance, in Hungary we applied a 10-km buffer around modelled maps to include the large flooded areas reported in reference maps and avoid overfitting. In England, we used a 5-km buffer due to the high density of the river network mapped in the official maps. For the Po river Basin, we excluded from the comparison the areas belonging to the Adige River Basin and the lowland drainage network, which are not included in the official hazard maps. In Spain and Norway official flood hazard maps have only been produced where relevant assets are at risk, according to available documentation [MITECO 2011; NVE 2020]. We therefore restricted the comparison only to areas where official flood hazard maps have been produced. Table 2 provide the list of parameters used to determine the areas used for the comparison.

Test area	**Buffer value (reference maps)**	**Buffer value (modelled maps)**
Hungary	NA	10 km
Po River Basin	NA	See main text
Norway	5 km	5 km
Spain	5 km	5 km
England	NA	5 km

Table 2. List of parameters used to determine the extent of areas used for comparing reference and modelled maps (NA: buffer not applied).

We evaluate the performance of simulated flood maps against reference maps using a number of indices proposed in literature (Bates and De Roo, 2000; Alfieri et al., 2014; Dottori et al., 2016b; Wing et al., 2017). The hit ratio HR evaluates the agreement of simulated maps with observations and it is defined as:

$$HR = (Fm \cap Fo)/(Fo) \times 100 \quad (2)$$

where $Fm \cap Fo$ is the area correctly predicted as flooded by the model, and Fo indicates the total observed flooded area. The formulation of the hit ratio does not penalize overprediction, which can be instead quantified using the false alarm ratio FAR:

https://doi.org/10.5194/essd-2020-313
Preprint. Discussion started: 12 January 2021

$$FAR = (Fm/Fo)/(Fm) \times 100 \quad (3)$$

where Fm/Fo is the area wrongly predicted as flooded by the model. Finally, a more comprehensive measure of the agreement between simulations and observations is given by the critical success index CSI, defined as:

$$CSI = (Fm \cap Fo)/(Fm \cup Fo) \times 100 \quad (4)$$

where $Fm \cup Fo$ is the union of observed and simulated flooded areas.

2.4 Additional tests

To choose the best possible methodologies and datasets to construct the flood hazard maps, we have performed a number of tests using recent input datasets as well as by alternative strategies to account for vegetation effects on elevation data.

2.4.1 Elevation data

It is well recognized that the quality of flood hazard maps strongly depend on the accuracy of elevation data used for modelling (Yamazaki et al., 2017). This is especially crucial for continental scale maps, since the quality of available elevation datasets is rarely commensurate to the accuracy required for modelling flood processes [Wing et al., 2017]. Moreover, high-resolution and accurate elevation data such as LIDAR-based DEMs cannot be used for reasons of consistency, given that these data are only available for few areas and countries.

The recent release of new global elevation models have the potential for improving the accuracy of large scale flood simulations, and hence the quality of flood hazard maps. Here, we test the use of the MERIT DEM (Yamazaki et al., 2017) within the proposed modelling approach and we compare the results with those obtained with CCM DEM. The MERIT DEM is based on the SRTM data, similarly to CCM DEM, however it has been extensively corrected and improved through comparisons from other large scale datasets, to eliminate error biases, to improve data accuracy at high latitudes (areas above 60° are not covered by SRTM) and compensate for factors like vegetation cover. Note that areas above 60° in CCM DEM were derived from national datasets, and therefore it is where the two datasets are likely to differ most.

2.4.2 Correction of elevation data with land use

https://doi.org/10.5194/essd-2020-313
Preprint. Discussion started: 12 January 2021

We performed additional simulations applying a method for correcting the CCM DEM elevation data based on land use. In fact, this dataset is mostly based on SRTM data and therefore elevation data can be wrongly increased due to the height of vegetation canopy in densely vegetated areas, and by buildings in urban areas. Specifically, we use the landuse map derived from Corine Land Cover and GlobCover to identify land uses corresponding to densely vegetated areas and urban areas, and we applied a correction factor as a function of local land use to locally reduce elevation. The correction factor varies from 8m for dense forested areas, to 2m for urban areas. Note that this values are based on the findings of previous literature studies such as Baugh et al. (2013) and Dottori et al. (2016b), while a formal calibration was not undertaken.

3) Results and discussion

We present the outcomes of the validation exercise by describing first the general results at country and regional scale in Section 3.1. Then, we discuss in the main text the outcomes for England, Hungary and Spain (Section 3.2), while the Norway and Po river basin case studies are presented in the Appendix B. We also complement the analysis with additional validation over major river basins in England and Spain. In Section 3.3 we compare our results with the validation exercise carried out by Wing et al. (2017) and with the findings of other literature studies. Finally, in Section 3.4 and 3.5 and Appendix B we compare the performance of the present and previous version of the flood map dataset, and we discuss the results of the tests with different elevation data and strategies to account for vegetation.

3.1 Validation of modelled maps at national and regional scale

Table 3 presents the results of the validation for each testing area and return period. The first visible outcome is the low scores for the comparisons with reference maps with high probability of flooding, i.e. low flood return periods (<30 years). Performances improve markedly with the increasing of return periods, with a general increase in the hit rate HR and decrease of false alarm rate FAR. In particular, critical success index (CSI) values approach 0.5 for the low probability flood maps, i.e., for return periods equal or above 500 years. Considering that most of the reference flood maps include the effect of flood defences (contrary to the modelled maps), these results suggest that the majority of rivers in the study areas may be protected for

https://doi.org/10.5194/essd-2020-313
Preprint. Discussion started: 12 January 2021

flood return periods around 100 years or lower, as indeed reported by available flood defence databases (Scussolini et al., 2016). The better performance for low-probability floods may also depend on floodplain morphology, where valley sides create a morphological limit to flood extent.

	RP	HR	FAR	CSI
Spain	10	0.58	0.65	0.28
Hungary	30	0.77	0.88	0.11
Spain	100	0.63	0.44	0.42
Hungary	100	0.76	0.74	0.24
Norway	100	0.70	0.72	0.25
England	100	0.53	0.31	0.43
Po River Basin	500	0.60	0.13	0.56
Spain	500	0.61	0.36	0.45
Hungary	1000	0.76	0.45	0.47
England	1000	0.52	0.12	0.48

Table 3. Results of the validation against official flood hazard maps: value of the performance indices at country and regional scale. RP=Return Period, HR=Hit Ratio, FAR= False Alarm Ratio, CSI=Critical Success Index.

3.2 Discussion of modelled maps at national and regional scale

The results in Table 2 highlight considerable differences in the skill of the flood maps across countries and regions. While some differences may arise from the variability of floodplain morphology and model input data, others are attributable to the different methods applied to produce the reference maps (MITECO 2011; NVE 2020). In the following sections we examine in more detail the outcomes for each study area.

3.2.1 England

According to Table 3, modelled flood maps tend to underestimate flood extent in England, as visible by the hit rate values around 0.5 (e.g. out of every two flooded cells, only one is correctly identified as flooded by the model). Such result is confirmed when focusing the

https://doi.org/10.5194/essd-2020-313
Preprint. Discussion started: 12 January 2021

analysis on the major river basins of England, as reported in Table 4. Notably, hit rates have generally marginal or no increases with the increase of return period considered, while FAR values have a marked decrease. The results of reported by Arnal et al. (2019) and summarized in Figure A1 suggest a fair hydrological skill of the LISFLOOD calibration in England, with KGE values generally above 0.5. However, there's not a clear correlation between hydrological and flood map skill, with some basins (e.g. Thames) showing high KGE values but relatively low CSI values.

Catchments	**100-year RP**			**1000-year RP**		
	HR	**FAR**	**CSI**	**HR**	**FAR**	**CSI**
England	**0.53**	**0.31**	**0.43**	**0.52**	**0.12**	**0.48**
Ouse	0.57	0.39	0.42	0.56	0.19	0.49
Severn	0.64	0.24	0.53	0.63	0.20	0.54
Thames, above Lea	0.56	0.46	0.38	0.55	0.23	0.47
Trent	0.63	0.28	0.50	0.59	0.06	0.57
Tyne	0.51	0.43	0.37	0.52	0.28	0.43

Table 4. Validation indices in England and in major river basins.

These results and the visual inspection of the reference maps suggest that the underestimation is mostly caused by the high density of mapped river network in the reference maps, in respect to modelled maps. Indeed, the modelling framework excludes river basins with an upstream basin area below 500 km^2, meaning that EFAS maps only cover main river stems but miss out several smaller tributaries. This is clearly visible over the Severn and in the upper Thames basins (Figure 4), and might also explain the lower skill in the lowlands of Ouse and Trent rivers, where the contributions of main river stems and tributaries to the flood extent are difficult to separate. Including minor tributaries in the flood maps would require either to increase the resolution of the climatological forcing to better reproduce intense local rainfall, or to add a pluvial flooding component as done by Wing et al. (2017). Furthermore, along river estuaries the skill of the modelled maps may be reduced by the absence of storm surge and tidal flooding components in the modelling framework.

https://doi.org/10.5194/essd-2020-313
Preprint. Discussion started: 12 January 2021

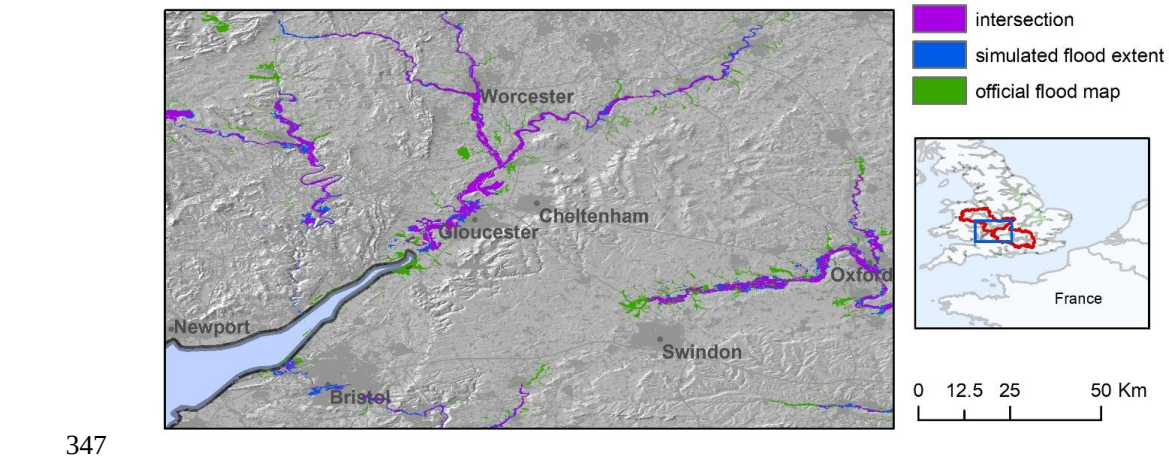

Figure 4. Comparison of modelled (blue) and reference (green) flood hazard maps (1-in-100-year) over the Severn (centre) and in the upper Thames basins in England (on the right). Purple areas denotes intersection (agreement) between the modelled and reference set of maps.

3.2.2 Hungary

The results in Table 3 for Hungary show a general tendency to overestimate flood extent for all return periods. Hit rate values are consistently high and do not change much with the return period. Conversely, false alarm rate is very high for the 1-in-30 year flood map and still considerable even for the 1-in-1000 year flood map. Arnal et al (2019) reported a fair hydrological skill of LISFLOOD (KGE values >0.5) for the calibration period, even though KGE validation values were considerably low for the Tisza River.

Given that flood defences are not modelled in reference maps, the observed results may be explained by assuming a large conveyance capacity of river channels. For instance, the 1-in-100 year reference map show relatively few flooded areas for the Danube main stem (Figure 5), thus suggesting that the main channels can convey the 1-in-100-year discharge without overflowing. Conversely, river channels in the modelling framework are assumed to convey only the 1-in-2-year discharge. Obviously, the same considerations can be made for 1-in-30-year discharge for the majority of river network, which explains the very low scores. Furthermore, artificial structures such as road embankments and drainage network may further reduce flood extent in lowland areas, leading to further overestimation given the fact that these features are not

https://doi.org/10.5194/essd-2020-313
Preprint. Discussion started: 12 January 2021

368 represented in the DEM. These findings highlight the need for high-resolution DEM fed with
369 local-scale information to achieve adequate performance in lowland areas, as observed also by
370 Wing et al (2019b).

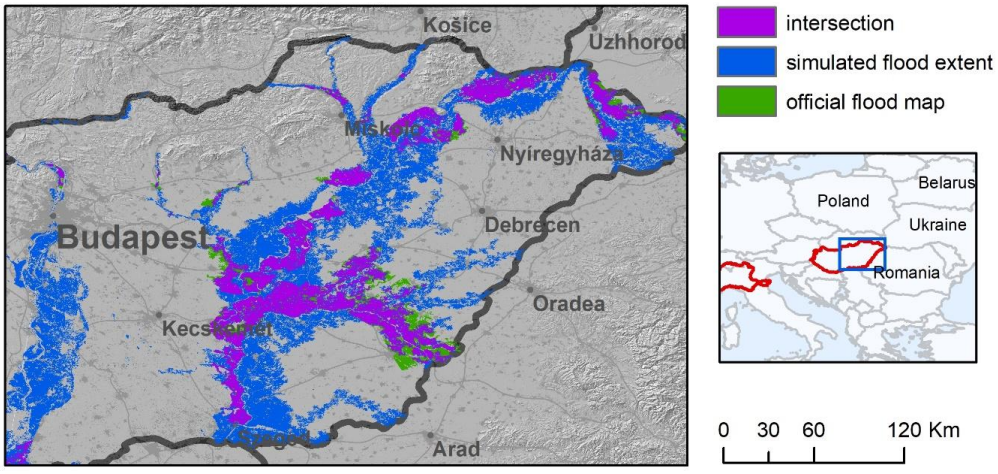

371

372 *Figure 5. Comparison of modelled (blue) and reference (green) flood hazard maps (1-in-100-*
373 *year) over the Danube (left) and Tisza (right) rivers in Hungary. Purple areas denotes the*
374 *intersection between the modelled and reference set of maps.*

375

376 ### *3.2.3 Spain*

377 The performance of the modelled maps in Spain show a fairly stable HR value and decreasing
378 FAR values with increasing return periods, similarly to what was observed for England and
379 Hungary. The analysis of the results for the major river basins of the Iberian Peninsula, reported
380 in Table 5, provide further insight on the skill of flood maps. A number of basins exhibit both
381 large HR and FAR such as the Duero, Tajo and Guadalquivir basins. Rivers in South-East Spain
382 (Segura, Jucar) have relatively low HR values, while the modelled maps perform better in the
383 Ebro river basin. The interpretation of results requires to consider different aspects. The poor
384 results for the 1-in-10-year maps are likely due to the effect of flood protection structures, such
385 as dykes and flood regulation systems, which are probably relevant also for the 1-in-100-year
386 map. Indeed, most Iberian rivers are regulated by multiple reservoirs, which are often used to
387 reduce flood peaks according to specific operating rules. While dykes are not represented in the
388 inundation model, reservoirs are included in the LISFLOOD model through a simplified

https://doi.org/10.5194/essd-2020-313
Preprint. Discussion started: 12 January 2021

approach, given that operating rules are not known. As such, the real and modelled hydrological regimes might differ significantly, including flow peaks of low-probability flood events. This is reflected also by the low hydrological skill of LISFLOOD, with KGE values generally below 0.5 with few exceptions (Figure A1).

In addition, the comparison of modelled and reference maps is partly affected by the partial coverage of the reference inundation maps in several river basins. According to the information available in the official website (MITECO 2011) large sections of the river network in the basins of the Duero, Tajo, Guadiana and Guadalquivir rivers have not been analyzed, due to the absence of relevant assets or inhabited places at risk. Even though this has been accounted by restricting the area of comparison around reference maps, a visual inspection of the maps being compared shows spurious overestimation around the edges of reference map polygons (Figure 6). Finally, the low HR values scored in rivers in South-East Spain (Segura, Jucar) are partially explained by the presence of several tributaries not included in EFAS maps.

Catchments	**10-year RP**			**100-year RP**			**500-year RP**		
	HR	**FAR**	**CSI**	**HR**	**FAR**	**CSI**	**HR**	**FAR**	**CSI**
Spain	**0.58**	**0.65**	**0.28**	**0.63**	**0.44**	**0.42**	**0.61**	**0.36**	**0.45**
Duero	0.60	0.74	0.22	0.65	0.55	0.36	0.65	0.46	0.42
Ebro	0.71	0.46	0.45	0.75	0.27	0.59	0.74	0.23	0.61
Guadalquivir	0.67	0.66	0.29	0.69	0.49	0.42	0.66	0.46	0.42
Guadiana	0.52	0.63	0.28	0.60	0.42	0.42	0.61	0.31	0.48
Jucar	0.32	0.89	0.09	0.53	0.46	0.36	0.51	0.39	0.39
Tajo	0.60	0.85	0.14	0.70	0.63	0.32	0.69	0.49	0.41
Segura	0.18	0.89	0.07	0.38	0.52	0.27	0.41	0.24	0.36

Table 5. Validation indices in Spain and in some test river basins.

https://doi.org/10.5194/essd-2020-313
Preprint. Discussion started: 12 January 2021

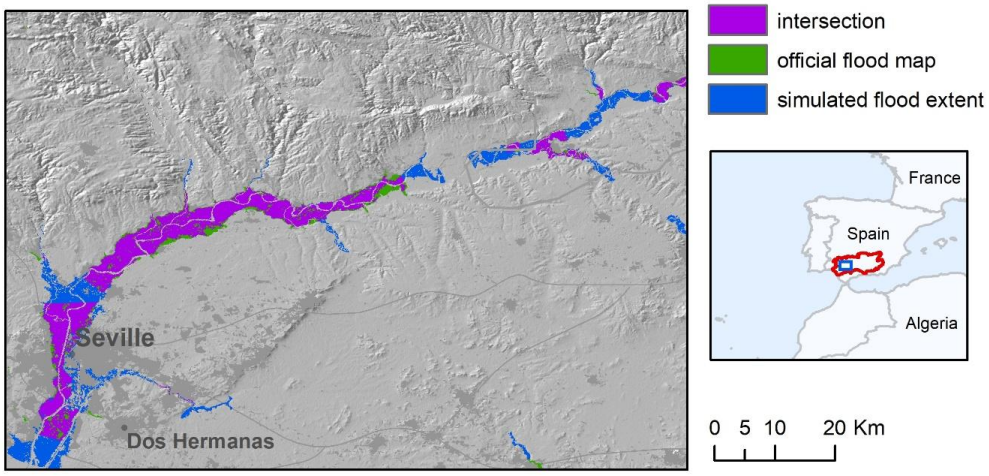

Figure 6. Comparison of modelled (blue) and reference (green) flood hazard maps (1-in-100-year) over a stretch of the Guadalquivir river basin, Spain. Purple areas denote the intersection between the two set of maps.

3.3 Comparison with previous continental-scale validation studies

To put the described outcomes in context, we compare them with the validation exercise performed by Wing et al. (2017) over United States, which is, to our knowledge, the only study that carried out a consistent validation of modelled flood hazard maps at continental scale. A comparison of validation indices of the two studies is shown in Table 6. For our framework, HR, FAR, CSI have been calculated by aggregating all areas with 100-year, 500-year and 1000-year reference maps.

As can be seen in Table 4, the continental-scale model by Wing et al. achieved the highest scores both for 100y and 500y return periods. However, this model is based on national datasets with higher accuracy and resolution than those available for the European continent (e.g. a 10m-resolution DEM and a detailed catalogue of flood defences). The global and European models have comparable hit rates for the 100-year flood maps (0.68 and 0.65 respectively), but the former exhibits a much lower FAR value (0.34 compared to 0.61 of the European model), and a higher HR value for the 500-year maps.

The higher HR values scored by the US and global models might depend on the higher density of the modelled river network, which includes river reaches up to 50km^2 by simulating both

https://doi.org/10.5194/essd-2020-313
Preprint. Discussion started: 12 January 2021

pluvial and fluvial flooding processes. The lower FAR values of the US and global models might be explained by the inclusion of flood defences. In the US model, defences are explicitly modelled using the US dataset of flood defences, while the global model parameterizes flood defences through the adjustment of channel conveyance using socioeconomic factors and degree of urbanization (Wing et al., 2017). However, Wing et al observed that the latter methodology had a negligible effect on hit rates in defended areas, when compared against an undefended version of the model.

Another possible reason for the low FAR values is the different approach used in the validation method. Wing et al. applied a narrow 1km buffer around official maps to constrain the area of comparison and avoid spurious over-prediction in areas not considered by official maps. However, this might result in a reduction of true false alarms, because part of overestimated flood areas can go undetected. To verify this hypothesis, we recalculated the performance indices against the 100-year reference map in Spain using a 1km buffer instead of the 5km previously applied to constrain the validation area. As a result the false alarm ratio dropped from 0.44 to 0.34, similar to the performance of the global model. However, we observed a reduction of true false alarms, especially in river basins with continuous map coverage such as the Ebro, Jucar and Segura.

	RP	**HR**	**FAR**	**CSI**
US model (Wing et al.)	100	0.82	0.37	0.55
Global model (Wing et al.)	100	0.69	0.34	0.50
European model (this study)	100	0.66	0.61	0.32
US model (Wing et al.)	500	0.86	na	na
Global model (Wing et al.)	500	0.74	na	na
European model (this study)	500	0.61	0.24	0.51
European model (this study)	1000	0.68	0.39	0.47

Table 6. Comparison of the performance indices for the European model described in the present study and the two models evaluated in the study by Wing et al. (2017).

To provide further context, the US model by Wing et al. (2017) attained average CSIs of ~0.75 against a number of detailed local models, whereas flood models built and calibrated for local

https://doi.org/10.5194/essd-2020-313
Preprint. Discussion started: 12 January 2021


Open Access Earth System Science Data Discussions

447 applications may achieve CSI scores up to 0.9 when benchmarked against very high quality data
448 (see Wing et al., 2019a). Fleischmann et al. (2019) recently proposed that regional-scale models
449 can provide locally relevant estimates of flood extent when CSI > 0.65. Although the overall
450 values shown in Table 3 are consistently below this threshold, better results are observed for a
451 number of river basins, as shown in Tables 4 and 5.
452

453 ### *3.4 Comparison with the previous flood map dataset*

454 Table 7 compares the performances of the flood hazard maps described in the present study
455 (version 2) with the previous version developed by Dottori et al. (2016a; version 1). The
456 comparison is shown for England and Hungary. Results for all other areas are comprised within
457 the range of results shown in Table 3. As can be seen, differences are generally reduced across
458 the different areas and return periods. Version 1 of the flood maps produced slightly better
459 results in Hungary for the 100- and 1000-year return period (increased CSI and HR, lower
460 FAR), while version 2 has somewhat improved performances in England, mainly driven by
461 higher HR.

	RP (y)	**F2/F1**	**ΔHR**	**ΔFAR**	**ΔCSI**
Hungary	30	0.97	-0.5%	-0.4%	2.9%
Hungary	100	1.00	-2.1%	0.7%	-2.4%
Hungary	1000	1.01	-3.6%	5.7%	-6.3%
England	100	1.05	9.4%	1.7%	7.3%
England	1000	1.04	8.2%	-1.1%	7.7%

462 *Table 7. Comparison of performances of the flood hazard maps described in the present study*
463 *and developed by Dottori et al. (2016a). Table reports the ratio between flood extents (F2/F1)*
464 *and the difference between version 2 and 1 of the HR,CSI,FAR values.*
465

466 These outcomes may be interpreted considering the changes in input data between the two
467 versions, and the structure of the modelling approach and of input data, which in turn has not
468 changed substantially. The main difference between the two map versions is given by the
469 hydrological input, with version 2 using the latest calibrated version of the LISFLOOD model.

https://doi.org/10.5194/essd-2020-313
Preprint. Discussion started: 12 January 2021

For the 100-year return period, peak flow values of version 2 are on average 35% lower than version 1 in Hungary, and 16% lower in England. However, similar decreases are also observed for the 1-in-2-year peak discharge which determines bankful discharge. The resulting reduction in channel hydraulic conveyance in respect to version 1 is likely to offset the decrease of peak flood volumes, which explain the small difference in overall flood extent given by the F2/F1 parameter in table 7. Such result confirm that the knowledge of river channel geometry is crucial to correctly model the actual channel conveyance and thus improve inundation modelling. Other differences in input data are given by minor changes in Manning's parameters and in the EFAS river network, which might contribute to the observed differences.

3.5 Influence of elevation data

Table 8 compares the indices calculated with CCM DEM elevation data against the same indices for the modelled flood maps based on MERIT-DEM. The comparison is carried out for England, Hungary and the Po river basin. Performance is slightly improved by the use of MERIT-DEM data for all areas and return periods, in particular through the reduction of FAR, even though the overall increase of CSI values is limited to few percentage points.

	RP (y)	**ΔF**	**ΔHR**	**ΔFAR**	**ΔCSI**
Hungary	100	-5.3%	0.0%	-2.0%	5.1%
Hungary	1000	-5.9%	-0.1%	-7.6%	5.2%
England	100	0.0%	2.6%	-5.7%	3.8%
England	1000	1.7%	2.8%	-7.8%	3.2%
Po	500	0.2%	0.9%	-4.3%	3.4%

Table 8. Comparison of performances of the flood hazard maps described in the present study and developed by Dottori et al. (2016a based on the MERIT-DEM (a) and CCM-DEM (b). Table reports the ratio between flood extents F and the differences for HR,CSI,FAR (e.g. (HRa-HRb)/HRa).

Because of this limited improvement and the considerable amount of time required to rerun the complete set of flood hazard maps (several days for each return period) it was decided not to

https://doi.org/10.5194/essd-2020-313
Preprint. Discussion started: 12 January 2021

494 update the flood maps using the MERIT-DEM as elevation data. Moreover, new high-resolution
495 datasets such as the Copernicus DEM (ESA-Airbus 2019) and MERIT-HYDRO (Yamazaki et
496 al., 2019) have recently become available, and therefore future research could focus on
497 performing additional comparisons to identify which dataset is most suitable for inundation
498 modelling in Europe.
499

500 *4) Conclusions and ongoing work*

501 We presented here a new dataset of flood hazard maps covering the geographical Europe and
502 including large parts of the Middle East and river basins entering the Mediterranean Sea. This
503 dataset significantly expands the previous available flood maps datasets at continental scale
504 (Alfieri et al., 2014; Dottori et al., 2016a), and therefore constitutes a valuable source of
505 information for future research studies and flood management, especially for countries where no
506 official flood hazard maps are available. The maps are being used for a range of applications at
507 continental scale, from evaluating present and future river flood risk scenarios, to the cost-
508 benefit assessment of different adaptation strategies to reduce flood impacts, and for
509 comparisons between different regions, countries and river basins (Dottori et al, 2020b).
510 Moreover, the flood hazard maps have been designed to be integrated with the European Flood
511 Awareness System (EFAS), and will be used to perform operational flood impact forecasting in
512 EFAS (Dottori et al., 2017).
513 We performed a detailed validation of the modelled flood maps in several European countries
514 against official flood hazard maps. The resulting validation exercise is the most complete
515 undertaken so far for Europe to our best knowledge, and provided a comprehensive overview of
516 the strengths and limitations of the new maps.
517 Modelled maps generally achieve low scores for high and medium probability of flooding. For
518 the 1-in-100-year flood probability, the modelled maps can identify on average two-thirds of
519 reference flood extent, however they also largely overestimate flood-prone areas in many
520 regions, thus hampering the overall performance. Performances improves markedly with the
521 increasing of return period, mostly due to the decrease of the false alarm rates. In particular,
522 critical success index (CSI) values approach and in some cases exceed 0.5 for return periods

https://doi.org/10.5194/essd-2020-313
Preprint. Discussion started: 12 January 2021

523 equal or above 500 years, meaning that the maps can correctly identify more than half of
524 flooded areas in the main river stems and tributaries of different river basins.
525 It is important to note that the validation was affected by problems in identifying the correct
526 areas for a fair comparison, because of the different density of the mapped river network in
527 reference and modelled maps. In our study we opted for a conservative approach using large
528 buffers to constrain comparison areas, which possibly penalized the model performance, e.g.
529 due to spurious false alarms in areas not considered by official map. However, we observed that
530 the proposed maps achieve comparable results to other large-scale flood models when using
531 similar parameters for the validation.
532 The low skill of modelled maps for high and medium probability of flooding, with large
533 overestimations observed in different lowland areas, is mostly motivated by the non-inclusion
534 of flood defences in the modelling framework and the simplified representation of channel
535 hydraulic conveyance, due to the absence of datasets at European scale describing river
536 channels and defence structures (i.e. design standards and location of dyke systems). Such
537 information combined with high-resolution DEM fed with local-scale information (artificial and
538 defence structures) is crucial to improve the performance of large-scale flood models and apply
539 more realistic flood modelling tools, as observed also by Wing et al (2017, 2019b). On this
540 point, we found that the modelling approach has limited sensitivity to changes in the
541 hydrological input, because channel conveyance is linked to streamflow characteristics. Such
542 finding highlight the need for independent data of river channel width, shape and depth to better
543 reproduce streamflow and flooding processes. Moreover, the improved results offered by the
544 use of the MERIT-DEM elevation data suggest that recent high-resolution datasets such as the
545 Copernicus DEM (ESA-Airbus 2019) and MERIT-HYDRO (Yamazaki et al., 2019) may offer a
546 viable solution to improve future versions of continental-scale flood hazard maps in Europe.
547 Increasing map coverage by including the minor river network is likely to improve the skill of
548 modelled maps. However, this might require the use of a different modelling approach to
549 account for pluvial flooding (Wing et al., 2017), along with reliable model climatology to
550 represent small-scale precipitation processes. Improving the simulation of reservoirs may also
551 reduce the difference between the real and modelled hydrological regimes in regions such as the
552 Iberian Peninsula and the Alps.
553

https://doi.org/10.5194/essd-2020-313
Preprint. Discussion started: 12 January 2021

554

555 *Data availability*

556 The dataset described in this manuscript is accessible as part of the data collection "Flood
557 Hazard Maps at European and Global Scale" at the JRC data Catalogue
558 (https://data.jrc.ec.europa.eu/collection/floods/).
559 Please refer to the dataset as follows: Dottori F., Bianchi A., Alfieri, L., Skoien, J., Salamon P.,
560 2020. River flood hazard maps for Europe and the Mediterranean Basin region. JRC Data
561 Catalogue, accessibile at https://data.jrc.ec.europa.eu/dataset/1d128b6c-a4ee-4858-9e34-
562 6210707f3c81 .
563 Note that the DOI for the dataset will be available soon. The dataset comprises the following
564 eight maps, each one available as GEOTIF file:

565 • Map of permanent water bodies for Europe and the Mediterranean Basin region
566 • River network in Europe and the Mediterranean Basin region
567 • River flood hazard maps for Europe and the Mediterranean Basin region (return periods of
568 10, 20, 50, 100, 200 and 500 years)

569 The official flood hazard maps used for the validation exercise are freely accessible at the
570 following websites:

571 • Spain: https://www.miteco.gob.es/es/cartografia-y-sig/ide/descargas/agua/zi-lamina.aspx
572 (in Spanish)
573 • Po River Basin: https://pianoalluvioni.adbpo.it/progetto-esecutivo-delle-attivita/ (in
574 Italian)
575 • Norway: https://www.nve.no/flaum-og-skred/kartlegging/flaum/ (in Norwegian)
576 • England: https://data.gov.uk/dataset/bed63fc1-dd26-4685-b143-2941088923b3/flood-
577 map-for-planning-rivers-and-sea-flood-zone-3 ; https://data.gov.uk/dataset/cf494c44-
578 05cd-4060-a029-35937970c9c6/flood-map-for-planning-rivers-and-sea-flood-zone-2
579 • Hungary: https://www.vizugy.hu/index.php?module=content&programelemid=62 (in
580 Hungarian)

581 The LISFLOOD hydrological model used in this research is released as open-source software
582 and available at https://ec-jrc.github.io/lisflood/.

https://doi.org/10.5194/essd-2020-313
Preprint. Discussion started: 12 January 2021

583 The LISFLOOD-FP hydrodynamic model used in this research can be requested to the authors
584 for research and non-commercial purposes at
585 http://www.bristol.ac.uk/geography/research/hydrology/models/lisflood/
586

587 # *Appendix A: LISFLOOD calibration results*

588 We report here the results of the LISFLOOD calibration presented by Arnal et al. (2019). The
589 hydrological skill of LISFLOOD is expressed by the Kling-Gupta Efficiency (KGE, Gupta et
590 al., 2009). Figure A1 shows the spatial distribution of the hydrological skill across the EFAS
591 domain. 75 % of all stations (543 out of 717) scored a KGE higher than 0.5 during calibration,
592 and 57 % (409 out of 698) during validation.
593 It is clearly noticeable that the skill is not homogeneously distributed across Europe, with higher
594 skills in large parts of Central Europe, and lower skill mostly in Spain caused by the strong
595 influence of reservoirs. The other study areas considered in the validation exercise (England,
596 Hungary, Norway, Po river basin) exhibit KGE values generally above 0.5.

597 # *Appendix B: Additional results*

598 ## *B1: validation results for the Po River Basin*

599 According to Table 3, the modelled flood maps provide a better reproduction of reference maps
600 for the Po River, compared to other study areas. False alarms are low, while hit ratio (HR)
601 values indicate that two out of every three pixels in the reference map are correctly identified as
602 flooded. The analysis of reference and modelled maps (Figure B1), suggests that the
603 underestimation is partly caused by flooded areas along some tributaries which are not included
604 in modelled maps. Other areas with omission errors are located near confluences of the Po main
605 stem and the major tributaries in Emilia-Romagna, which may depend on the underestimation of
606 peak flow on tributaries. In fact, the results of the LISFLOOD calibration in Figure A1 show
607 better hydrological skill along the Po main stem, compared to some tributaries. Finally, it is
608 likely that the inclusion of smaller tributaries of the river network in the modelled maps would
609 improve the overall performance.
610

https://doi.org/10.5194/essd-2020-313
Preprint. Discussion started: 12 January 2021

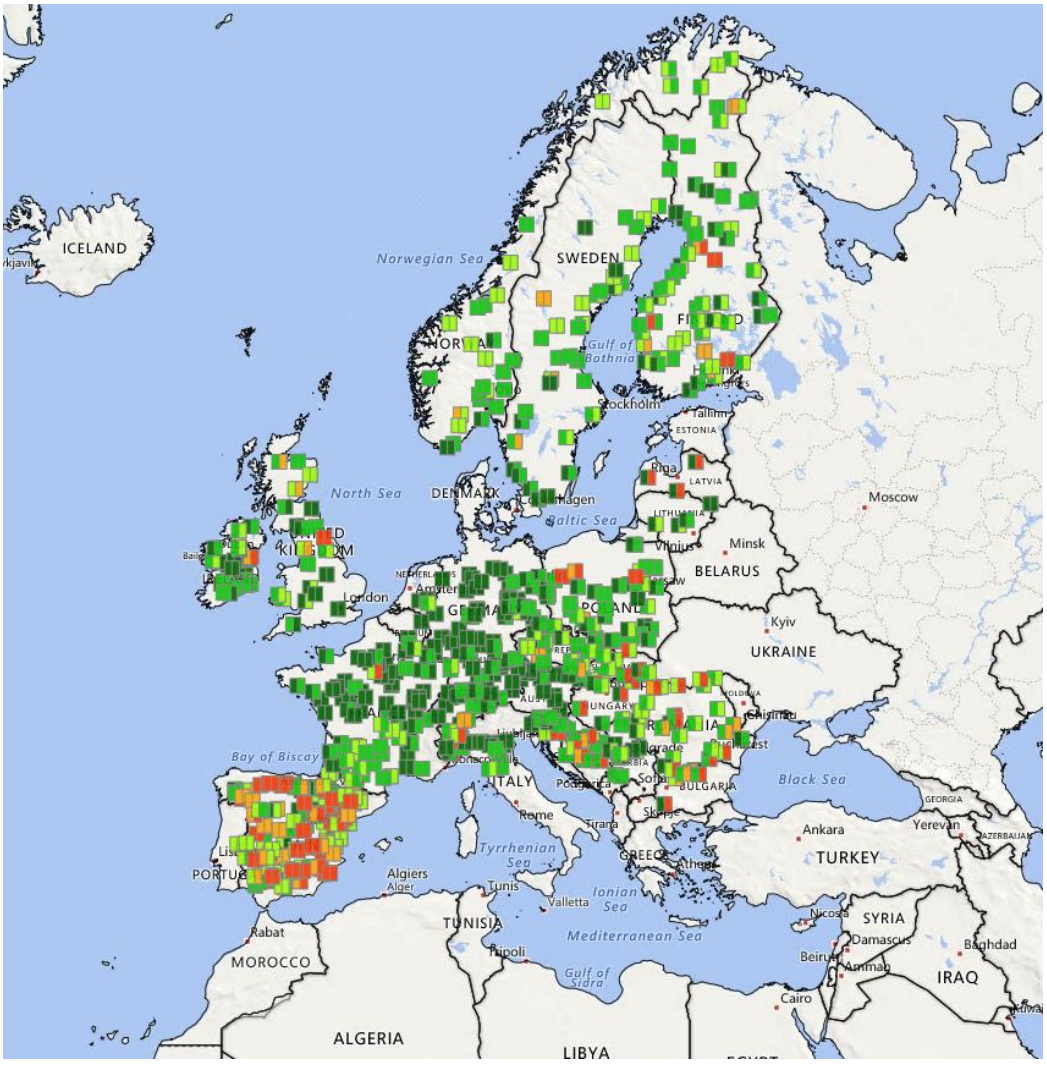

611

612 *Figure A1. Hydrological skill of EFAS at the calibration locations. Colour coding denotes the*
613 *quality of the KGE during calibration (left half of square) and validation (right half of the*
614 *square). Dark green: KGE > 0.75; Green: KGE 0.5 – 0.75, Light green: KGE 0.2 – 0.5;*
615 *Orange: 0 – 0.2; Red: < 0. Source: Arnal et al. (2019).*

616

https://doi.org/10.5194/essd-2020-313
Preprint. Discussion started: 12 January 2021

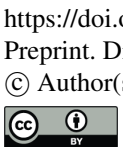

Open Access Earth System Science Data Discussions

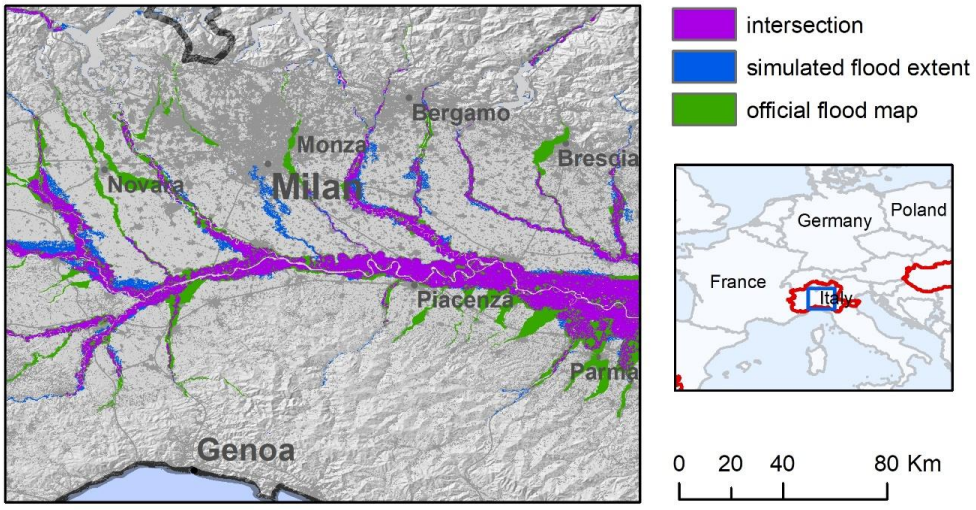

Figure B1. Comparison of modelled (blue) and reference (green) flood hazard maps (1-in-500-year) over the Po river basin, Italy. Purple areas denotes the intersection (agreement) between the two set of maps.

B2: validation results for Norway

The results of the modelled flood maps in Norway show a general tendency to overestimate flood extent for the 1-in-100-year events, with high values for both hit ratio (HR) and false alarm ratio (FAR). Such a result is in fact largely influenced by the relatively small extent and discontinuous coverage of reference maps. Flood-prone areas for the 1-in-100-year official maps only cover 215 km^2, possibly due to the low density of populated places in Norway, while they cover between 4700 and 5700 km^2 for England, Spain and Hungary. As for Spain, we applied a 5km buffer to restrict the area of comparison around reference maps, yet this leads to spurious overestimation around the edges of reference map polygons. Notably, the performance improves markedly with the use of a 1km buffer as in Wing et al., (2017), which results in increased critical success index (CSI) scores up to nearly 0.50.

The results of reported by Arnal et al. (2019) and summarized in Figure A1 suggest an acceptable hydrological skill of the LISFLOOD calibration in Norway, with a majority of gauge stations scoring KGE values above 0.5. In the areas with lower scores, the model performance for low-probability flood events might be influenced by an incorrect estimation of peak

https://doi.org/10.5194/essd-2020-313
Preprint. Discussion started: 12 January 2021

discharges driven by snow melt, which plays a relevant role in determining low-probability flood events.

B3) Influence of correcting elevation data with land use

We tested the results of correcting CCM DEM elevation data with vegetation cover in Scandinavia, where the percentage of land covered by forests is more relevant than in the other regions included in the modelled flood maps. For the 1-in100-year flood maps, the overall difference in flood extent between the corrected and uncorrected maps is less than 4%, and similar values were found for the other return periods. Moreover, the HR, FAR and CSI values of two set of maps differ by less that 2% when calculated against the 1-in100-year official map in Norway, probably because forested areas have not been considered as relevant flood-prone areas. These results suggest that the simulation of densely vegetated areas have a limited importance in determining the overall performance of modelled flood maps in Europe.

Author contribution

FD: conceptualization, formal analysis, investigation, data curation writing (original draft, review and editing); LA: methodology, investigation, writing (review and editing); AB: data curation, validation, visualization; JS: investigation, writing (review and editing); PS: conceptualization, project administration, writing (original draft, review and editing)

Competing interests

The authors declare that they have no conflict of interest.

Acknowledgements

This study has been partially funded by the COPERNICUS programme and by an administrative arrangement with Directorate General 'European Civil Protection and

https://doi.org/10.5194/essd-2020-313
Preprint. Discussion started: 12 January 2021

Open Access Earth System Science Data Discussions

664 Humanitarian Aid Operations (DG ECHO) of the European Commission. EFAS is operated and
665 financed as part of the Copernicus Emergency Management Service.
666
667

https://doi.org/10.5194/essd-2020-313
Preprint. Discussion started: 12 January 2021

References

Alfieri, L., Salamon, P., Bianchi, A., Neal, J., Bates, P.D., Feyen, L., 2014. Advances in pan-European flood hazard mapping, Hydrol. Process.,28 (18), 4928-4937, doi:10.1002/hyp.9947.

Alfieri L., Feyen L., Dottori F., Bianchi A., 2015. Ensemble flood risk assessment in Europe under high end climate scenarios. Global Environmental Change 35, 199–212.

Alfieri, L., L. Feyen, and G. D. Baldassarre (2016), Increasing flood risk under climate change: a pan-European assessment of the benefits of four adaptation strategies, Clim. Change, 136(3), 507–521, doi:10.1007/s10584-016-1641-1.

Arnal, L., S.-S. Asp, C. Baugh, A. de Roo, J. Disperati, F. Dottori, R. Garcia, M. GarciaPadilla, E. Gelati, G. Gomes, M. Kalas, B. Krzeminski, M. Latini, V. Lorini, C. Mazzetti, M. Mikulickova, D. Muraro, C. Prudhomme, A. Rauthe-Schöch, K. Rehfeldt, P. Salamon, C. Schweim, J.O. Skoien, P. Smith, E. Sprokkereef, V. Thiemig, F. Wetterhall, M. Ziese, 2019. EFAS upgrade for the extended model domain – technical documentation, EUR 29323 EN, Publications Office of the European Union, Luxembourg, 2019, ISBN 978-92- 79-92881-9, doi: 10.2760/806324, JRC111610.

Bates, P. D., De Roo, A. P. J., 2000. A simple raster-based model for flood inundation simulation, J. Hydrol., 236 (1–2), 54–77.

Bates P.D., Horritt M.S., and Fewtrell T.J., 2010. A simple inertial formulation of the shallow water equations for efficient two-dimensional flood inundation modelling. Journal of Hydrology, 387, 33-45.

Baugh, C. A., BatesP. D.,Schumann G., Trigg, M.A., 2013. SRTM vegetation removal and hydrodynamic modeling accuracy, Water Resour. Res. 49, 5276–5289, doi:10.1002/wrcr.20412.

Barredo JI, de Roo A, Lavalle C. 2007. Flood risk mapping at European scale. Water Science and Technology 56: 11–17.

Bontemps, S., et al., 2009. GLOBCOVER -Products description and validation report, Univ. Catholique de Louvain.

Burek, P., Knijff van der, J., Roo de, A., 2013. LISFLOOD, Distributed Water Balance and Flood Simulation Model Revised User Manual 2013. Publications Office, Luxembourg.

Copernicus Land Monitoring Service. Corine Land Cover. http://land.copernicus.eu/pan-european/corine-land-cover (accessed on 12/2/2020).

https://doi.org/10.5194/essd-2020-313
Preprint. Discussion started: 12 January 2021

698 Dottori, F., Alfieri, L., Salamon, P., Bianchi, A., Feyen, L., Lorini, V., 2016a: Flood hazard
699 map for Europe - 100-year return period. European Commission, Joint Research Centre (JRC)
700 [Dataset] PID: http://data.europa.eu/89h/jrc-floods-floodmapeu_rp100y-tif
701 Dottori, F., Salamon, P., Bianchi, A., Alfieri, L., Hirpa, F.A., Feyen, L., 2016b.
702 Development and evaluation of a framework for global flood hazard mapping. Advances in
703 Water Resources 94, 87–102.
704 Dottori F., Kalas M.,Salamon P., Bianchi A., Alfieri, L., Feyen L., 2017. An operational
705 procedure for rapid flood risk assessment in Europe. Nat. Hazards Earth Syst. Sci., 17, 1111-
706 1126, https://doi.org/10.5194/nhess-17-1111-2017.
707 Dottori, F., Szewczyk, W., Ciscar, J.C., Zhao, F., Alfieri, L., Hirabayashi, Y., Bianchi, A.,
708 Frieler, K., Betts, R.A., Feyen, L., 2018 Increased human and economic losses from river floods
709 with anthropogenic warming. Nature Climate Change, 8(9), 781-786,
710 https://doi.org/10.1038/s41558-018-0257-z
711 Dottori F., Bianchi A., Alfieri, L., Skoien, J., Salamon P., 2020a. River flood hazard maps
712 for Europe and the Mediterranean Basin region. JRC Data Catalogue, accessibile at
713 https://data.jrc.ec.europa.eu/dataset/1d128b6c-a4ee-4858-9e34-6210707f3c81 .
714 Dottori F, Mentaschi L, Bianchi A, Alfieri L and Feyen L, 2020b. Adapting to rising river
715 flood risk in the EU under climate change, EUR 29955 EN, Publications Office of the European
716 Union, Luxembourg, 2020, ISBN 978-92-76-12946-2 , doi:10.2760/14505, JRC118425.
717 European Commission (EC), 2007. Directive 2007/60/EC of the European
718 Parliament and of the Council on the assessment and management of flood risks,
719 Official Journal of the European Communities, Brussels, available at: http://eur-
720 lex.europa.eu/legal-content/EN/TXT/?uri=CELEX%3A32007L0060 (accessed on 13/5/2020).
721 ESA-Airbus, 2019. Copernicus Digital Elevation Model Validation Report, accessed on
722 14/5/2020 at https://spacedata.copernicus.eu/documents/12833/20611/GEO1988-
723 CopernicusDEM-RP-001_ValidationReport_V1.0/9bc5d392-c5f2-4118-bd60-db9a6ea4a587
724 Feyen L, Dankers R, Bódis K, Salamon P, Barredo JI. 2012. Fluvial floodrisk in Europe in
725 present and future climates. Climatic Change: 112(1): 47–62, doi:10.1007/s10584-011-0339-7.
726 Fleischmann A., R. Paiva, W. Collischonn, 2019. Can regional to continental river
727 hydrodynamic models be locally relevant? A cross-scale comparison. Journal of Hydrology X,
728 2019.

https://doi.org/10.5194/essd-2020-313
Preprint. Discussion started: 12 January 2021

729 Gupta, H.V., H. Kling, K.K. Yilmaz, G.F. Martinez, 2009: Decomposition of the mean
730 squared error and NSE performance criteria: implications for improving hydrological
731 modelling. Journal of Hydrology, 377, 80-91.
732 Hirpa, F.A.; Salamon, P.; Beck, H.E.; Lorini, V.; Alfieri, L.; Zsoter, E.; Dadson, S.J. , 2018.
733 Calibration of the Global Flood Awareness System (GloFAS) using daily streamflow data. J.
734 Hydrol., 566, 595–606.
735 Jongman, B., Hochrainer-Stigler, S., Feyen, L., Aerts, J.C.J.H., Mechler, R., Botzen,
736 W.J.W., Bouwer, L.M., Pflug, G., Rojas, R., Ward, P.J., 2014. Increasing stress on disaster-risk
737 finance due to large floods. Nat. Clim. Change 4, 264-268,
738 doi:http://dx.doi.org/10.1038/nclimate2124.
739 Ministerio de Medio Ambiente y Medio Rural y Marino (MITECO), 2011. Guía
740 Metodologica para el desarrollo del sistema nacional de cartografia de zonas inundables.
741 Accessed on 18/5/2020 at https://www.miteco.gob.es/es/agua/temas/gestion-de-los-riesgos-de-
742 inundacion/snczi/Guia-metodologica-determinacion-zonas-inundables/default.aspx (in Spanish).
743 The Norwegian Water Resources and Energy Directorate, 2020. Flood Zone Maps.
744 Accessed on 24/4/2020 at https://www.nve.no/flaum-og-skred/kartlegging/flaum/ (in
745 Norwegian)
746 Paprotny, D., Morales-Nápoles, O., and Jonkman, S. N.: Efficient pan-European river flood
747 hazard modelling through a combination of statistical and physical models, Nat. Hazards Earth
748 Syst. Sci., 17, 1267-1283, https://doi.org/10.5194/nhess-17-1267-2017, 2017.
749 Sampson, C. C., Smith, A. M., Bates, P. D., Neal, J. C., Alfieri, L., & Freer, J. E. (2015). A
750 high-resolution global flood hazard model. *Water Resources Research*, *51*(9), 7358-7381.
751 Scussolini, P., Aerts, J. C. J. H., Jongman, B., Bouwer L. M., Winsemius H. C., de Moel H.,
752 and Ward, P. J., 2015. FLOPROS: an evolving global database of flood protection standards.
753 Nat. Hazards Earth Syst. Sci. Discuss., 3, 7275–7309, 2015, doi:10.5194/nhessd-3-7275-2015.
754 Thielen J., Bartholmes J., Ramos M.H., and De Roo A. (2009). The European flood alert
755 system - part 1: concept and development. Hydrol. Earth Syst. Sci. 13, 125-140.
756 Trigg, M. et al., 2016. The credibility challenge for global fluvial flood risk analysis.
757 Environ. Res. Lett.11 094014
758 United Nations Office for Disaster Risk Reduction (UNISDR), 2015. Sendai Framework for
759 Disaster Risk Reduction 2015–2030 (www.unisdr.org/we/inform/publications/43291)

https://doi.org/10.5194/essd-2020-313
Preprint. Discussion started: 12 January 2021

760 Van der Knijff, J.M., Younis, J., de Roo, A.P.J., 2010. LISFLOOD: a GIS-based
761 distributedmodel for river basin scale water balance and flood simulation. Int. J. Geogr. Inf. Sci.
762 24, 189-212.
763 Vogt et al., 2007. A pan-European river and catchment database, JRC Reference Reports,
764 doi:0.2788/35907.
765 Ward, P.J. et al., 2015. Usefulness and limitations of global flood risk models. Nature
766 Climate Change 5, 712–715.
767 Wing, O. E., Bates, P. D., Sampson, C. C., Smith, A. M., Johnson, K. A., & Erickson, T. A.
768 (2017). Validation of a 30 m resolution flood hazard model of the conterminous United States.
769 Water Resources Research, 53(9), 7968-7986, doi:10.1002/2017WR020917.
770 Wing, O. E. J., Sampson, C. Bates, P. D., Quinn, N., Smith, A. M., Neal, J. C., C. (2019a).
771 A flood inundation forecast of Hurricane Harvey using a continental-scale 2D hydrodynamic
772 model. Journal of Hydrology X 4 , 100039.
773 Wing, O. E. J., Bates, P. D., Neal, J. C., Sampson, C. C., Smith, A. M., Quinn, N., et al.
774 (2019b). A New Automated Method for Improved Flood Defense Representation in Large-Scale
775 Hydraulic Models. Water Resources Research 55, 11007-11034, https://doi.org/2019WR025957
776 Yamazaki, D., Ikeshima, D., Tawatari, R., Yamaguchi, T., O'Loughlin, F., Neal, J.,
777 Sampson, C., Kanae, S., Bates, P. D. (2017). A high accuracy map of global terrain elevations.
778 Geophysical Research Letters.
779 Yamazaki, D., Ikeshima, D., Sosa, J., Bates, P. D., Allen, G. H., & Pavelsky, T. M. (2019).
780 MERIT Hydro: a high-resolution global hydrography map based on latest topography dataset.
781 Water Resources Research, 55, 5053–5073. https://doi.org/10.1029/2019WR024873
782 Zuzanna Zajac, Z:, Zambrano-Bigiarini, M., Salamon, P., Burek, P., Gentile, A., Bianchi,
783 A., 2013. Calibration of the LISFLOOD hydrological model for Europe. JRC technical report
784 JRC87717.